The Adosrption Study for the Removal of Rhodamine-B from Artificial Aquatic Solution by using Activated *Hygrophila auriculata* Nano Carbon

M. AJITHKUMAR[1] and S. ARIVOLI[1]*

[1]PG and Research Department of Chemistry, Poompuhar College(AU),
(Affiliated to Bharathidasan University), Melaiyur-609107, Tamilnadu, India.
*Corresponding author E-mail: arivu6363@gmail.com, ajimurugan1996@gmail.com

ABSTRACT

To study the adsorption of Rhodamine-B dye (Rh-B) from artificial aquatic solution by using activated *Hygrophila auriculata* nano carbon under batch adsorption mode. Activated nano carbon was synthesized from *Hygrophila auriculata* and it was characterised by analytical methods such as BET(BJH), XRD, FTIR, and SEM with EDX. The equilibrium adsorption data were calculated and it was interrelated using Freundlich, Langmuir, Temkin, Hurkins-Jura, Halsay, Radlich-Peterson, Dubinin-Radushkevich, Jovanovic, and Brunauer Emmett Teller (BET) isotherm models. The kinetics of the adsorption technique was examined via pseudo-second order, Elovich mode and intraparticle diffusion methods. Thermodynamic parameters like change of free energy ($\Delta G°$), change of enthalpy ($\Delta H°$), and change of entropy ($\Delta S°$) has been estimated. The value of regression coefficient (R^2) indicates that Langmuir isotherm suitable to designate the process. The maximum adsorption capacity of monolayer is 204.11 mg/g at 40°C. Based on the R^2 value the adsorption mechanism was fitting to the pseudo-second order model. Thermodynamic factors obtained ($\Delta G°$ ranged from -4429.50 to -640.26 kJ/mol; $\Delta H°$ ranged from 5.38 to 12.84 kJ/mol; and $\Delta S°$ ranged from 19.82 to 50.23 J/K/mol, correspondingly) representing the Rh-B dye removal from artificial aquatic solutions by AHANC is there spontaneous, endothermic and possible in nature respectively. The outcomes point out that AHANC could be used as low-price and an effective adsorbent for the removal of Rh-B dye from artificial aqueous solution.

Keywords: Activated *Hygrophila auriculata* activated nano carbon (AHANC), Rhodamine-B dye (Rh-B), Adsorption isotherms, Equilibrium Kinetics, Thermodynamic parameters.

INTRODUCTION

The industries have been growing tremendously over the past few years. The consequence is the release of wastewater from factories into the environment without treatment. Water resources are highly polluted due to such kind of wastewater. Metals and organic dyes are often the main causes of water pollution, and also it is impossible for the dyes to decompose very easily. Aquatic organisms and micro-organisms are also affected due to its adverse effects and

thus human beings are pushed to the worst condition by the food chain. The removal of dyes is important for the wastewater treatment[1,2]. The conventional techniques based on the biochemical, physical, and chemical properties which are employed to remove dyes from aqueous solution by process of adsorption, flocculation, chemical oxidation, reverse osmosis, chemical precipitation, photocatalytic degradation, ion exchange and membrane filtration. However, adsorption technology has much attraction for its advantages such as simplicity, eco-friendliness and recyclability of adsorbents. The activated carbons have been widely functional an adsorbents for removal of dyes due to its low cost and efficiency[3-5].

The review literature displays that not at all used activated *Hygrophila auriculata* nano carbon in place of an adsorbent to remove water pollutants from the artificial aqueous solution. Present work, adsorption of organic dye such as Rh-B dye into activated nano carbon prepared by carbonation of Hygrophila auriculata with sulfuric acid. The amount and rate of adsorption of Rh-B dye were measured using AHANC from the aqueous solution by batch method. The obtained equilibrium isotherms and kinetics of adsorption data were used to illustrate the efficiency of adsorbent.

METHODOLOGY

Rhodamine-B dye solution

Analytical grade (AR) chemicals are used on this experiment were obtained from Sree Sabari Scienntifics in Mayiladuthurai, Tamilnadu-606 001. The stock solution of Rh-B was made at 1000 ppm by stirring constantly at room temperature in order to liquefy the dye molecules completely using deionized water. The experimental solution was prepared by diluting the 1000ppm solution to required concentration. The physicochemical properties of adsorbate (Rh-B) are listed in Table 2 (a).

Synthesis of AHANC

The *Hygrophila auriculata* is used as an adsorbent in this research work and it is collected from nearby Poompuhar, Mayiladuthurai, Tamilnadu–609 107. The stem of *Hygrophila auriculata* is washed by purified water to eliminate

mud also dust then dried using hot-air-oven at 110°C. Then, carbonization of the *Hygrophila auriculata* stem was adding w/v ratio Con. Sulfuric acid to get the primary carbon. In that point activated to 6 h at 1000°C in muffle furnace in direction of obtain AHANC. The physico chemical properties of adsorbent (AHANC) are listed in Table 2(b).

Table 1: Nomenclature

%R	-Percentage of removal of Rh-B (%)
C_0	- Initial concentration of Rh-B (mg/L)
C_t	-Concentration at time 't' of Rh-B (mg/L)
C_e	-Equilibrium concentration of Rh-B (mg/L)
q_e	-Quantity of adsorbed Rh-B at equilibrium (mg/L)
υ	-Volume of solution Rh-B (L)
w	-AHANC weight (g)
K_f	-Adsorption capacity of Freundlich (L/mg)
n_F	-Adsorption intensity of Freundlich
q_m	-Maximum Rh-B removal (mg/g)
K_L	-Adsorption capacity of Langmuir (L/mg)
R_L	-Dimensionless constant Separation factor
R	-Gas constant of (8.314 J/K/mol)
T	-Temperature (K)
b_T	-Connected to sorption heat (J/mol)
K_T	-Temkin isotherm constant (L/g)
B_H & A_H	-Harkin Jura isotherm constants
K_{Ha} & n_{Ha}	-Halsey isotherm constants
G	-Radlich Peterson isotherm exponent
K_R	-Redlich Peterson isotherm constant (L/g)
q_D	-Dubinin-Radushkevich isotherm saturation capacity (mg/g)
B_D	-Dubinin-Radushkevich isotherm constant (mol²/kJ²)
ε	-Potential of Polanyi (J/mol)
q_J	-Jovanovich maximum adsorbate uptake (mg/g)
K_J	-Jovanovich constant (L/g)
C_{BET}	-Surface binding energy (L/mg)
q_s	-BET isotherm saturation capacity theoretically (mg/g)
C_s	-Adsorbate monolayer saturation (mg/L)
q_t	-Amount of adsorbed Rh-B at any time (mg/g)
k_2	-Pseudo-second order rate constant for adsorption (g/mg/min)
T	-Time (min)
H	-Pseudo second order initial adsorption rate (mg/g min)
A	-Rate of initial adsorption (mg/g/min)
B	-Elovich model constant (g/mg)
R^2	-Correlation co-efficient
k_{id}	-Intra-particle diffusion rate constant (mg/g/min$^{1/2}$)
α	-Constant that depicts the adsorption mechanism
K_o	-Thermodynamic constant at equilibrium
C_{solid}	-Concentration at equilibrium for solid phase (mg/L)
C_{liquid}	-Concentration at equilibrium for liquid phase (mg/L)
ΔH^0	-Change in enthalpy (kJ/mol)
ΔS^0	-Change in entropy (J/mol/K)
ΔG^0	-Change in Gibbs free energy (kJ/mol)
E_a	-Energy of activation (KJ/mol)
Θ	-Surface coverage
S*	-Sticking probability

Table 2(a): Character table of Rh-B

Name (IUPAC)	[9-(2-carboxyphenyl)-6-diethylamino-3-xanthenylidene]-diethylammonium chloride
Another name	Rhodamine-610
Dye type	Cationic dye
Chemical formula	$C_{28}H_{31}ClN_2O_3$
Molar mass (g/mol)	479.02
Appearance	Red to violet powder

Table 2(b): Character table of AHANC

Name	Activated Hygrophila auriculata Nano Carbon
Diameter (nm)	116.5
Surface Area (m²/g)	90.067
Micropore volume (cc/g)	0.257
Micropore area (m²/g)	636.727
pHZPC	6

Characterization performances

The particle diameter, surface area, micro pore volume, micro pore area, frequency of function groups, molecular arrangements, surface morphology and elemental compositions of the adsorbent was analysed by using the following instrumentations such as particle analyzer, Brunauer Emmett Teller (BET), Spectroscopy of Fourier Transform Infrared (FTIR), X-Ray Diffraction (XRD), Scanning Electron Microscope (SEM) with Energy Dispersive X-ray (EDX).

Experimental procedure of batch adsorption

The adsorption experiments had been finished in a batch method[6] at 303, 313, 323 and 323K. The noted weight of AHANC was added into 50 mL of the experimental Rh-B solution with 25ppm of initial concentration at known pH. The stuffing were shaken using a motorized shaker rotary with 120rpm until equilibrium reached. Then the solution was filtered at fixed time and then measured the Rh-B concentration of tested solution using UV Visible spectrometer at 554 nm. An amount of adsorbed Rh-B as well as the removal percentage of Rh-B can be calculated as following relationships in equation 1 and 2.

Mass Balance Relationship	Equation	Eq. No.
Percentage of removal	$\% R = \left(\dfrac{C_0 - C_t}{C_0}\right) \times 100$	(1)
Amount of adsorption	$q_e = v \times \dfrac{(C_0 - C_e)}{w}$	(2)

Active parameters
Interactive time

The influence of interactive time[7] among the AHANC and adsorbate for to remove the Rh-B from artificial aquatic solution is determined by keeping origin dye concentration, adsorbent dose, pH, in addition temperature as constant using at different time intervals.

Dose of adsorbent

The different doses comprising of the AHANC respectively mixed with Rh-B solutions and the subjects are rotated in motorized shaker. The capacities of adsorption for different dose is determined at certain time intervals by keeping all other constraints are constant.

Origin pH

The experiment of adsorption process was carried out in between pH solutions of 3 and 9. Acidic and basic pHs of solution kept by adding the mandatory volume of dil. HCl and dil. NaOH solution. Even though factors of interactive time, adsorbent dose, temperature and Rh-B dye concentration were kept constant throughout the experiment.

Other ionic strength

Adsorption of Rh-B tested experimentally in the presence of chloride ion. This leads to resolve the percentage of Rh-B adsorbed from 25 ppm of origin concentration of Rh-B solution through changing concentration of the added chloride ion keeping all other factors are constant.

Adsorption isotherm

Adsorption isotherms[8] designate exactly how adsorbate molecules assign among the solid and aquatic phase at the minute of adsorption process which extends to an equilibrium state. Quite a lot of isotherms had been used in the adsorption study to define experimental information of adsorption isotherms. Designed at this study, the following isotherm models such as; Freundlich, Langmuir, Temkin, Hurkins-Jura, Halsay, Radlich-Peterson, Dubinin-Radushkevich, Jovanovic and Brunauer-Emmett-Teller isotherm. These equations of isotherm models are given in equation 3 to 11 respectively.

Isotherm Models	Linear Equation	Plot	Eq. No.
Freundlich	$log q_e = log K_F + \dfrac{1}{n_F} log C_e$	$log q_e$ Vs. $log C_e$	3
Langmuir	$\dfrac{C_e}{q_e} = \dfrac{1}{q_m K_L} + \dfrac{C_e}{q_m}$	$\dfrac{C_e}{q_e}$ Vs. C_e	4
	$R_L = \dfrac{1}{1 + K_L C_0}$		4(i)
Temkin	$q_e = \dfrac{RT}{b_T} \ln K_T + \dfrac{RT}{b_T} \ln C_e$	q_e Vs. $\ln C_e$	5
Hurkins Jura	$\dfrac{1}{q_e^2} = \dfrac{B_H}{A_H} - \dfrac{1}{A_H} log C_e$	$\dfrac{1}{q_e^2}$ Vs. $log C_e$	6
Halsay	$ln q_e = \dfrac{ln K_{Ha}}{n_{Ha}} - \dfrac{ln C_e}{n_{Ha}}$	$ln q_e$ Vs. $ln C_e$	7
Radlich Peterson	$ln \dfrac{C_e}{q_e} = g ln C_e - ln K_R$	$ln \dfrac{C_e}{q_e}$ Vs. $ln C_e$	8
Dubinin Radushkevich	$ln q_e = ln q_D - B_D \varepsilon^2$	$ln q_e$ Vs. ε^2	9
Jovanovic	$ln q_e = ln q_J - K_J C_e$	$ln q_e$ Vs. C_e	10
Brunauer Emmett Teller(BET)	$\dfrac{C_e}{q_e(C_s - C_e)} = \dfrac{1}{q_s C_{BET}} + \left(\dfrac{C_{BET} - 1}{q_s C_{BET}}\right)\left(\dfrac{C_e}{C_s}\right)$	$\dfrac{C_e}{q_e(C_s - C_e)}$ Vs. $\left(\dfrac{C_e}{C_s}\right)$	11

Kinetics studies

Kinetics is the most important physical characteristic in its efficiency of an adsorption machanism[9]. Many parameters are generally well thought out in the study of adsorption process kinetics. Three recognized kinetic models, such as the pseudo-second order, Elovich, and intra-particle diffusion method are used to represent dynamic of adsorption mechanism. Equations for these operating models are given in equation 12 to 14.

Kinetic Models	Linear Equation	Plot	Eq. No.
Pseudo-second order	$\dfrac{t}{q_t} = \dfrac{1}{K_2 q_e^2} + \left(\dfrac{1}{q_e}\right) t$	$\dfrac{t}{q_t}$ Vs. t	12
Elovich model	$q_t = \dfrac{1}{\beta} \ln(\alpha\beta) + \dfrac{1}{\beta} ln t$	q_t Vs. $ln t$	13
Intra-particle diffution	$log\% R = log K_{id} + \alpha$ $log t$	$log\%R$ Vs. $log t$	14

Thermodynamics estimation

The state function of thermodynamics such as free energy change, enthalpy change and entropy change are significant pointers when evaluating the mechanisms of the adsorption mechanism[10]. Thermodynamic factors obtained using the given equations are 15 and 16.

Thermodynamic Models	Linear Equation	Plot	Eq. No.
Vant Hoff's equation	$\Delta G0 = - RT ln K_o$	$ln K_o$ Vs. $\dfrac{1}{t}$	16
	$ln K_o = \dfrac{\Delta S^0}{R} - \dfrac{\Delta H^0}{RT}$		
	$K_o = \dfrac{C_{solid}}{C_{liquid}}$		
Modified Arrhenius equation	$ln(1 - \theta) = ln S^* + \dfrac{E_a}{RT}$	$ln(1 - \theta)$ Vs. $\dfrac{1}{t}$	17
	$\theta = 1 - \dfrac{C_o}{C_e}$		

RESULTS AND DISCUSSIONS

BET, XRD, FTIR, SEM and EDX studies

Physical parameters such as particle size, area-surface, volume-pore and micropore area for adsorbent (AHANC) were determined using particle analyzer and BET (BJH) method and this data provided by Table 2(b). The XRD analysis of AHANC was shown in Fig. 1(a), strong and weak peaks emerged at $2\theta = 25$ and $2\theta = 40$ respectively.

This result indicates that the adsorbent structure nature for crystalline and bear a resemblance to the structure of graphite. The FT-IR model was an important tool to identify some significant frequencies of functional groups on the adsorbent, which are capable of adsorbing the adsorbate. The FTIR spectrometer was measured the wavenumber range 500 to 4000 cm^{-1} for AHANC and it's shown in Fig. 1(b). The peak frequency point; 2500 to 4000 cm^{-1} specifies single bond (Carbon-Hydrogen, Oxygen-Hydrogen, Nitrogen-Hydrogen), 2000 to 2500 cm^{-1} specifies triple bond (Carbon=Carbon, Carbon=Nitrogen), 1500 to 2000 cm^{-1} specifies double bond (Carbon=Carbon, Carbon=Nitrogen, Carbon=Oxygen) and 500 to 1500 cm^{-1} specifies the area of the fingerprint region. The SEM image

is charity for the morphological analysis of AHANC and porous structure of AHANC of SEM image shown in Fig. 1(c). The chemical composition of adsorbent was determined by EDX analysis, the EDX results shown as Fig. 1(d) as well as data presented in Table 3.

Table 3: The EDX result of AHANC

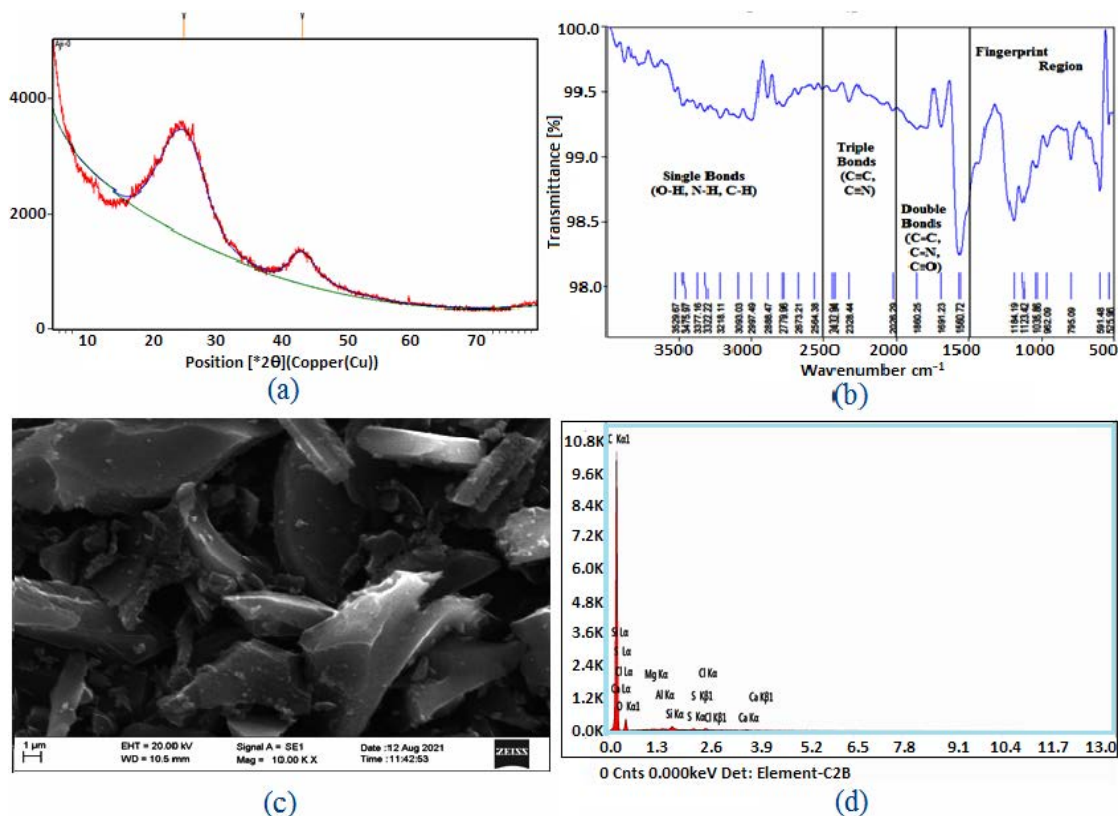| Elements	Mass(%)	Atom(%)	Errors(%)	Kratio
C K	85.60	89.70	4.40	0.595
O K	11.70	9.20	13.90	0.013
Mg K	0.50	0.20	13.20	0.002
Al K	0.40	0.20	13.20	0.002
Si K	0.70	0.30	7.20	0.005
S K	0.30	0.10	18.30	0.002
Cl K	0.40	0.10	19.90	0.003
Ca K	0.40	0.10	27.70	0.003

Fig. 1. (a) XRD of AHANC, (b) FTIR of AHANC, (c) SEM image of AHANC, and (d) EDX of AHANC

Effect of active parameters
Influence of interactive time

Influence of interactive time[11] was examined at 25 ppm of Rh-B solution, 25 mg of AHANCdose, 303 K and known pH. As can be seen in Fig. 2(a), while contact time was increases, the adsorption was not significantly increases. The removal of Rh-B occurred very hastily at the starting

of the experiment duration of first 30 min, then marginal increases up to 60 minute. The maximum removal of Rh-B onto AHANC was observed, it can be said that at beyond that there is almost no further increases in removal of the Rh-B in addition is therefore fixed because the equilibrium contact time and the equilibrium data have been presented in the Table 4.

Table 4: Equilibrium parameters for adsorption of Rh-B dye onto AHANC

C_0	C_e				q_e				%Removal			
	303K	313K	323K	333K	303K	313K	323K	333K	303K	313K	323K	333K
25	5.25	4.94	4.21	4.20	39.50	40.13	41.57	41.60	79.00	80.26	83.15	83.20
50	13.65	12.60	11.59	9.45	72.70	74.79	76.81	81.09	72.70	74.79	76.81	81.09
75	25.29	22.89	19.95	18.48	99.43	104.21	110.10	113.03	66.28	69.47	73.40	75.35
100	36.84	33.69	31.96	29.97	126.32	132.62	136.09	140.05	63.16	66.31	68.04	70.03
125	54.60	52.71	51.54	48.48	140.80	144.59	146.91	153.04	56.32	57.84	58.77	61.21

Influence of adsorbent dose

This experiment was voted for out to observe the effect of AHANC dose on removal of Rh-B from aquatic solution. The result obtained as shown in Fig. 2(b), this one can be realistic the elimination of the Rh-B increases by way of increasing AHANCdose as follows: 10, 25, 50, 100, 200, and 250 mg in 50 mL test solution AHANC, which is readily available and easily accessible to the Rh-B. The dye removal percentage increase was not significant when the AHANCdose increasing after 25 mg. At this point it was expected that concentrations of Rh-B on the surface of AHANCwould be high. The AHANCdose of 25 mg was considered optimal for future studies and its corresponding efficiency of removal was found as 83%.

Influence of origin pH

The Rh-B solution pH has been widely used because of its essential parameter in the adsorption process. The functional groups of AHANC surface are control for the interaction between the Rh-B with AHANC. The adsorbent can be added H^+ or added OH^- to different charges surface in solution at various pH. Therefore, the effect of pH of origin solution was studied in the pH range of 3 to 9 on removal of Rh-B from the artificial aquatic solution. The percentage removal increased from about 46% to 83% while slowly decreasing after pH 6, which is pH-ZPC (zero point charge) shown in Fig. 2(c). The pH-ZPC of AHANC is a very significant characteristic that controls the pH at surface has net neutral. At lower pH values (pH<pHzpc), the surface of AHANC can take on a positive charge, for that intention increases the adsorption of Rh-B due to the electrostatic force of an adsorbent as a support for maximum adsorbing Rh-B from the aquatic solution as resulting initial pH was optimized to pH 6.
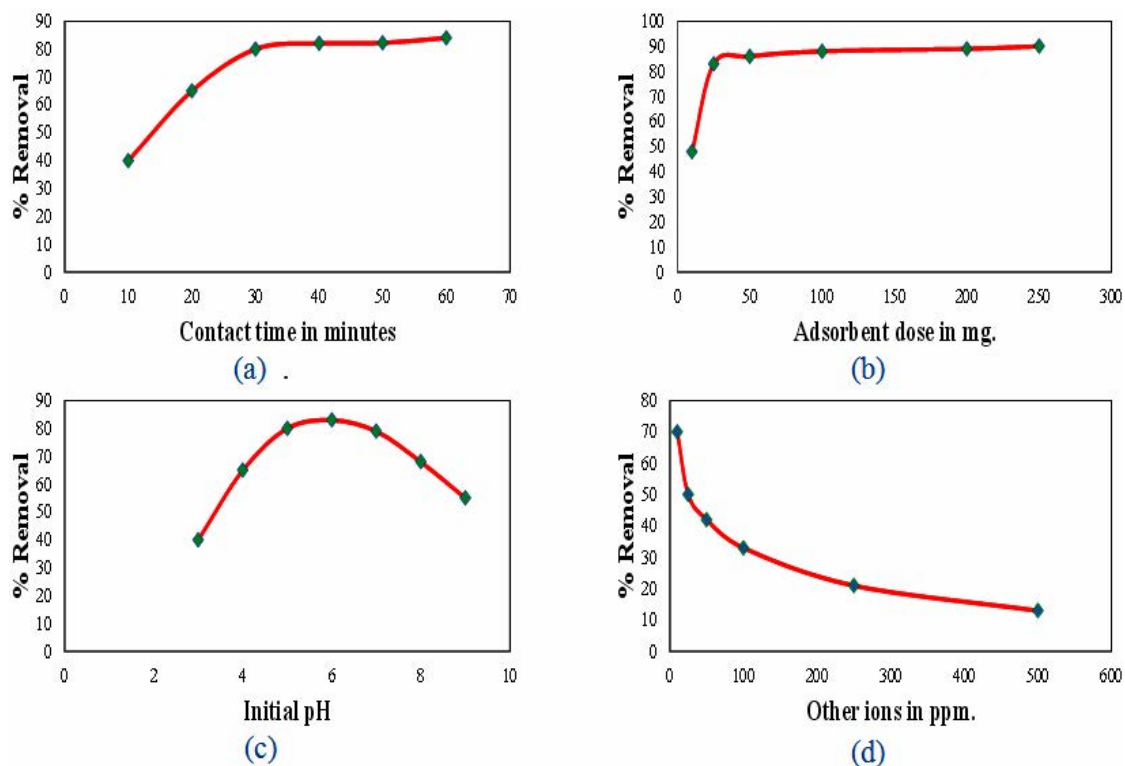

Fig. 2(a). Influence of interactive time on Rh-B removal, (b) Influence of adsorbent dose on Rh-B removal, (c) Influence of origin pH on Rh-B removal, and (d) Influence of other ionic strength on Rh-B removal

Influence of other ionic strength

As shown in Fig. 2(d), Rh-B adsorption onto AHANC is less when small amounts of NaCl solution are added. The influence of strength of ionic for adsorbing of Rh-B onto surface of AHANC was investigated in different concentrations of NaCl solution with 60 min of contact time, 25 mg adsorbent dose and 50 mL Rh-B solution with 25 ppm. If the electrostatic forces among the AHANC surface and Rh-B were striking, increases in the ionic strength would theoretically reduce the adsorption capacity, for this reason the competition of the dye molecules, Na^+ and Cl^- ions, investigational data commencing this work follow this agreement, as the removal of Rh-B onto AHANC decreased with the addition of NaCl solution[12].

Isotherm of Adsorption

The equilibrium of adsorption Rh-B could be quantified using recognized adsorption isotherms[13]. The parameters achieved from the various isotherms; provided essential statistics about the adsorption mechanism of Rh-B in addition onto surface, properties and empathies of AHANC. The experimental data were tested with the Freundlich, Langmuir, Temkin, Hurkins-Jura, Halsay, Radlich-Peterson, Dubinin-Radushkevich, Jovanovic and Brunauer-Emmett-Teller isotherm; in addition, the plots were given in Fig. 3(a-i), respectively. The isotherm parameters were given in Table 5 and regression coefficients is commonly used in determining the supreme of appropriate isotherm for removing Rh-B onto AHANC, at that point applicability of the isotherms is compared using the correlation coefficient rule. From this sustainability of the isotherms, the indispensable properties of Langmuir isotherm could be communicated with the method of the Dimensionless Separation Factor Constant (RL) by the equation 4(i).

Table 5: Parameter of Isotherms for adsorption of Rh-B onto AHANC

| Model	Constant	T (K)			
		303	313	323	333
Freundlich	K_f (mg/g) (L/mg)$^{1/n}$	16.36	17.32	20.71	21.75
	n_F	1.80	1.79	1.90	1.87
	R^2	0.99	0.98	0.97	0.95
Langmuir	q_m (mg/g)	199.51	204.11	195.66	203.37
	K_L (L/mg)	0.04	0.05	0.06	0.07
	R^2	0.99	0.99	0.99	1.00
Temkin	b_T (J/mol)	57.01	56.53	60.38	59.10
	K_T (L/mg)	0.43	0.45	0.57	0.60
	R^2	0.99	0.99	0.98	0.99
Hurkins Jura	A_H (g^2/L)	-1733.07	-1803.66	-2042.39	-2105.27
	B_H (mg^2/L)	-1.67	-1.64	-1.62	-1.59
	R^2	0.86	0.84	0.84	0.77
Halsay	K_{Ha} (mg/L)	154.85	162.94	316.72	316.05
	n_{Ha}	1.80	1.79	1.90	1.87
	R^2	0.99	0.98	0.97	0.95
Radlich Peterson	g	0.45	0.44	0.47	0.46
	K_R (L/g)	0.06	0.06	0.05	0.05
	R^2	0.99	0.97	0.97	0.94
Dubinin Radushkevich	q_D (mg/g)	115.44	120.57	123.13	131.80
	B_D (mol^2/kJ^2)	-5.79E-06	-4.98E-06	-3.45E-06	-3.44E-06
	R^2	0.86	0.87	0.86	0.92
Jovanovic	K_J (L/g)	0.02	0.02	0.02	0.03
	q_J (mg/g)	45.55	48.22	52.54	54.76
	R^2	0.83	0.79	0.75	0.72
BET	C_{BET} (L/mg)	-13.65	-59.11	-33.84	15.80
	q_s (mg/g)	36.65	45.31	49.48	65.80
	R^2	0.73	0.69	0.75	0.68
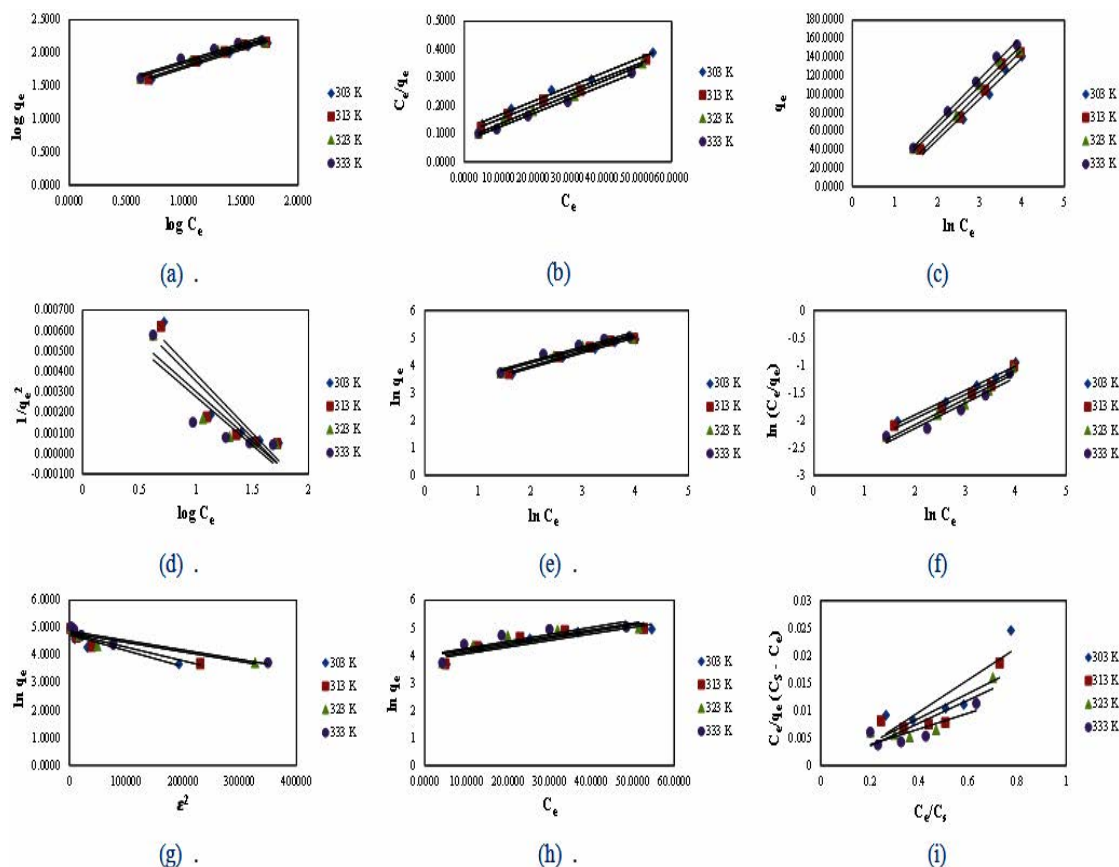
Fig. 3. Isotherm models for removal of Rh-B; (a) Freundlich, (b) Langmuir, (c) Temkin, (d) Hurkins-Jura, (e) Halsay, (f) Radlich-Peterson, (g) Dubinin-Radushkevich, (h) Jovanovic, and (i) Brunauer-Emmett-Teller (BET)

The parameter R_L indicates the dimensionless constant separation factor. $R_L > 1$ stands negative adsorption; $0 < R_L < 1$ stands fortunate adsorption; $R_L = 0$ stands irrevocable adsorption; $R_L = 1$ stands in lines adsorption. The R_L values in the middle of 0 to 1 indicate fortunate adsorption for all original concentration (C_o) and temperature calculated. The deliberate R_L values are specified in the Table 6.

Table 6: Rh-B adsorption onto AHANC of Dimensionless Separation Factor (RL)

| C_o | Temperature °C | | | |
	303 K	313 K	323 K	333 K
25	0.48	0.45	0.39	0.37
50	0.31	0.29	0.24	0.23
75	0.23	0.22	0.18	0.17
100	0.19	0.17	0.14	0.13
125	0.15	0.14	0.11	0.11

Kinetics studies

Quite a lot of steps can be used to study the mechanisms of control the adsorption mechanism like diffusion mechanism, mass transmission and chemical reaction; the kinetic models[14] ware used to investigate data of Rh-B adsorption onto AHANC. The kinetics of Rh-B adsorption onto AHANC is essential to select ideal functioning circumstances for the large-scale batch adsorption. Kinetic factors, useful for the estimate of the adsorption rate, provide essential statistics for design with modeling Rh-B adsorption. As a result, adsorption kinetics Rh-B adsorption onto AHANC were investigated using plots of the pseudo-second order, Elovich model and intra-particle diffusion kinetic models shown as Fig. 4 (a-e), 5 (a-e), and 6 (a-e), correspondingly as a specific concentrations, and these data provided in Table 7.

The correlation coefficients of pseudo-second order kinetic model were near to unity, leading to certainty of pseudo-second order model as long as a good correlation for the removal of Rh-B onto AHANC. The Elovich model indicate initial adsorption (α) increasing with temperatures,

similarly to t the initial adsorption rate (h) in pseudo-second order kinetic model. This could be because

of the boom with inside the pores or the energetic active Centre at the AHANC adsorbent.

Table 7: Kinetics factors for adsorbing Rh-B dye onto AHANC

C_0	T (K)	Pseudo-Second Order				Elovich Model			Intraparticle Diffusion		
		q_e	k_2	R^2	h	α	β	R^2	α	K_{id}	R^2
25	303	63.72	3.87E-04	0.95	1.57	3.19	6.84E-02	0.96	5.38E-01	8.45	0.99
	313	59.38	5.24E-04	0.96	1.85	3.73	7.27E-02	0.96	4.80E-01	10.91	0.99
	323	53.85	9.13E-04	0.98	2.65	5.94	8.52E-02	0.96	3.67E-01	17.98	0.98
	333	53.78	9.21E-04	0.98	2.66	6.00	8.55E-02	0.96	3.65E-01	18.12	0.98
50	303	96.06	4.40E-04	0.94	4.06	9.07	4.77E-02	0.91	3.83E-01	14.30	0.95
	313	94.83	5.42E-04	0.96	4.88	11.66	4.99E-02	0.93	3.45E-01	17.40	0.96
	323	96.91	6.42E-04	0.98	6.03	14.74	4.93E-02	0.95	3.26E-01	20.34	0.96
	333	93.25	8.68E-04	0.97	7.55	29.39	6.07E-02	0.88	2.47E-01	28.04	0.92
75	303	117.02	6.04E-04	0.96	8.28	30.30	4.75E-02	0.85	2.58E-01	21.72	0.89
	313	124.13	6.76E-04	0.99	10.42	35.52	4.37E-02	0.94	2.60E-01	23.96	0.95
	323	134.26	5.48E-04	0.99	9.87	27.28	3.75E-02	0.97	2.93E-01	22.15	0.98
	333	129.51	8.97E-04	1.00	15.05	59.74	4.42E-02	0.99	2.34E-01	29.54	0.98
100	303	151.80	5.85E-04	1.00	13.47	34.56	3.24E-02	0.97	2.94E-01	19.68	0.96
	313	158.03	5.58E-04	1.00	13.94	37.83	3.18E-02	0.99	2.87E-01	20.99	0.98
	323	159.77	6.19E-04	1.00	15.80	46.92	3.26E-02	0.98	2.69E-01	23.23	0.97
	333	163.43	6.32E-04	1.00	16.88	53.54	3.26E-02	0.98	2.60E-01	24.85	0.97
125	303	174.25	2.97E-04	0.93	9.00	22.52	2.77E-02	0.86	3.33E-01	13.40	0.91
	313	178.51	2.96E-04	0.93	9.42	24.01	2.73E-02	0.86	3.28E-01	14.10	0.91
	323	176.70	3.39E-04	0.94	10.60	30.33	2.89E-02	0.86	2.98E-01	16.21	0.90
	333	185.12	3.07E-04	0.93	10.52	28.61	2.70E-02	0.84	3.10E-01	16.01	0.89

Then it is depend on the fact that rate controlling step could be intra-particle diffusion. Furthermost widely used method for ascertaining the

mechanism intricate in adsorption mechanism is to use intra-particle diffusion model, which perform an vital role in adsorbing Rh-B to AHANC.
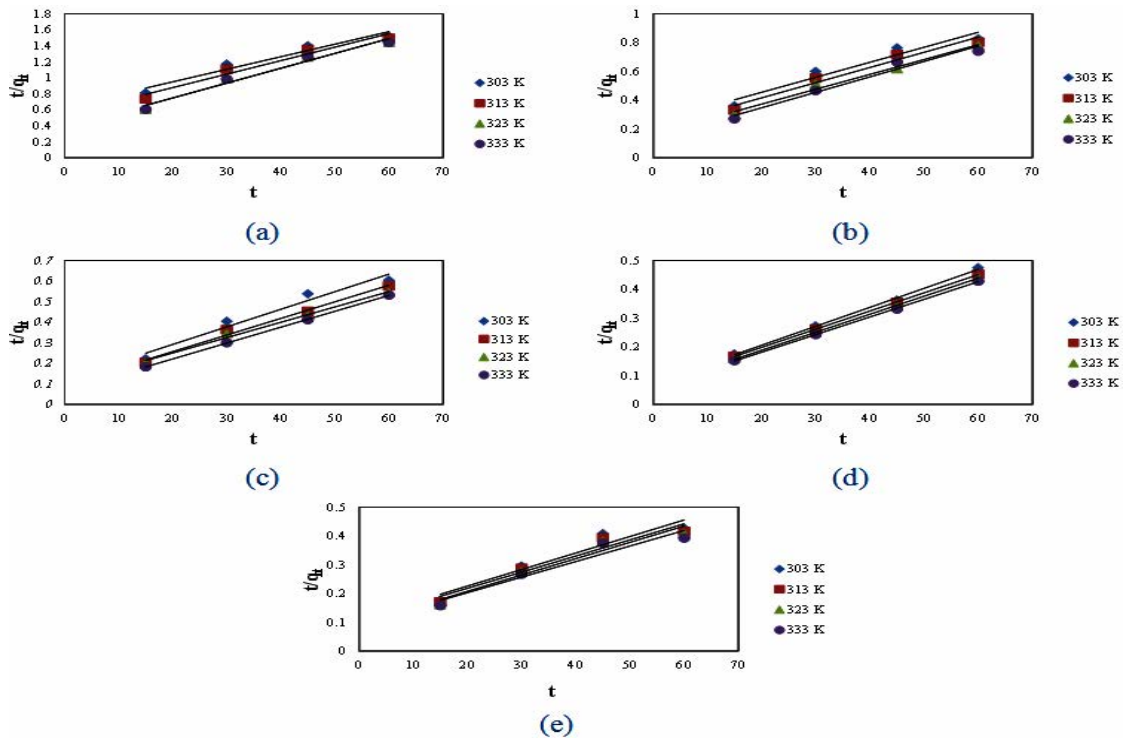

Fig. 4. Pseudo second order model; (a) 25ppm, (b) 50ppm, (c) 75ppm, (d) 100ppm, and (e) 125ppm
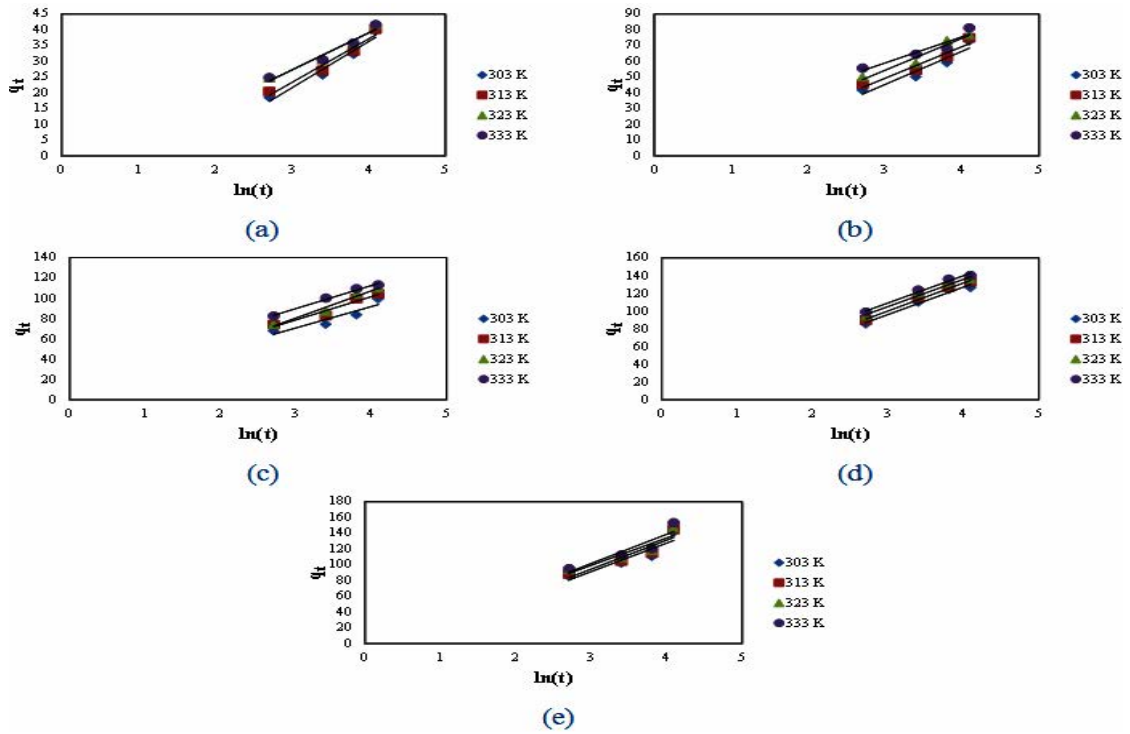
Fig. 5. Elovich model; (a) 25ppm, (b) 50ppm, (c) 75ppm, (d) 100ppm, and (e) 125ppm
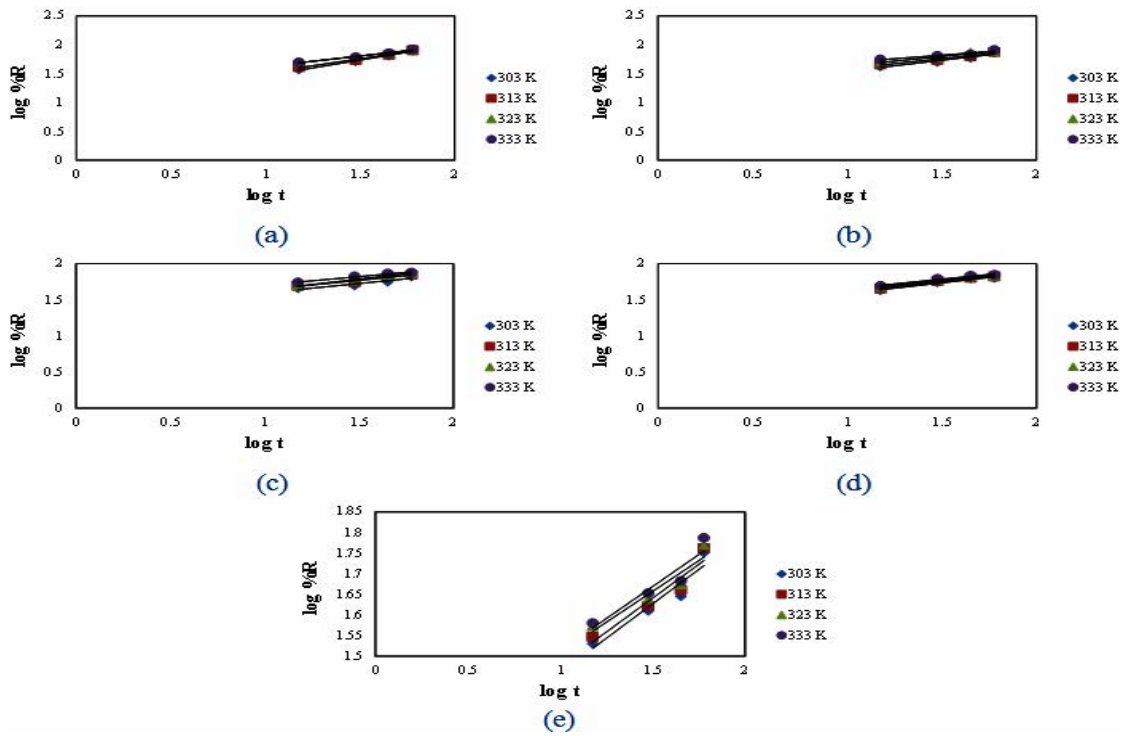

Fig. 6. Intra-particle diffusion model; (a) 25ppm,(b) 50ppm, (c) 7ppm, (d) 100ppm, and (e) 125ppm

Thermodynamic estimation

The thermodynamic parameters[15] relating to adsorption, through the standard Gibbs free energy change ($\Delta G°$), standard enthalpy

change (ΔH°) and standard entropy change (ΔS°) were intended and specified in the Table 8. Datas of ΔS° and ΔH° could be achieved by the slope and intersection of a line graph between lnKo and 1/T shown in Fig. 7(a). The ΔG° is negative values at different temperatures show the possibility of the process and the spontaneity

of adsorption. The change of the enthalpy of adsorption for physisorption is between 20 and 40 (kJ mol1). The positive values of ΔH° reveal adsorption is endo-thermic as well as physical nature. In addition, the positive values of ΔS° specify to raise uncertainty of AHANC/Rh-B solution during adsorption.

Table 8: Adsorption of Rh-B dye onto AHANCof Thermodynamic Parameters

C_0	ΔG°				ΔH°	ΔS°	Ea	S*
	303K	313K	323K	333K				
10	-3337.68	-3650.02	-4286.65	-4429.50	8.58	39.32	6970.31	1.32E-02
20	-2467.39	-2829.88	-3216.37	-4031.55	12.84	50.23	9877.61	5.56E-03
30	-1702.95	-2140.06	-2725.70	-3094.11	12.74	47.67	9046.67	9.32E-03
40	-1358.23	-1762.24	-2029.64	-2349.10	8.46	32.51	5641.86	3.90E-02
50	-640.26	-822.37	-951.41	-1263.38	5.38	19.82	3162.62	1.25E-01

Were calculated the energy of activation (Ea) and the probability of adhesion (S*) by the graph between ln(1-Θ) and 1/T, it was shown in the Fig. 7(b) also values given in Table 8. Positive values of Ea designate adsorption was endo-thermic nature, the

agreement through ΔH° positive values. The probability of sticking (S*) values are less than unity, which designate that the possibility of Rh-B ions onto AHANC surface was enormous as long S*<<<1 so, as these values authorize the sorption was physical adsorption.

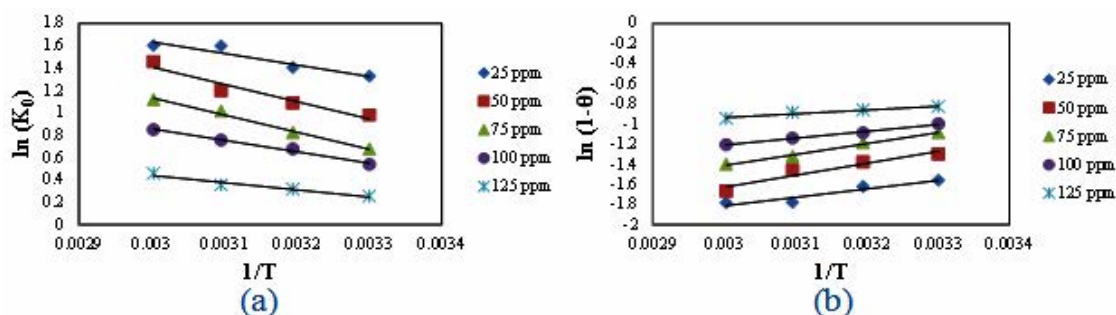**Fig. 7. (a) Vant Hoff's Plot, and (b) Plot of Activation energy (Ea) and Sticking probability(S*)**

Performance comparison

Table 9, summarizes the adsorption capacity, at an optimum volume and pH of the various adsorbents. In this present study, the high comparable capacity

for Rh-B adsorption is 204.11 mg/g for AHANC. This maximum removal of Rh-B dye reflects the maximum superficial active site for adsorption matched with former adsorbent resources listed in Table 9.

Table 9: Assessment of different adsorbent adsorption capacities

S.No	Adsorbent	q_m (mg/g)	Reference
1	-Ligno Sulfonate Fe_3O_4 Cr(VI)	022.47	[16]
2	-Furfural Residue (FR)	037.93	[17]
3	-ZIF-67/AC	046.20	[18]
4	-Polyamide Branches Grafted onto Carbon Microspheres	019.90	[19]
5	-NiO/SiO_2 nanocomposites	068.00	[20]
6	-Activated Hygrophila auriculata nano carbon (AHANC)	204.11	Present study

CONCLUSION

Results of this research work; conventional the possibility, low cost, obtainability, ease of planning and eco-friendly nature of activated Hygrophila auriculata nano carbon (AHANC) as a

promising and maintainable adsorbent for efficient Rh-B removal from aquatic solution. Adsorption was highly influenced through various effective factors, such as: interactive time, adsorbent dose, origin pH, and other ionic strength. The maximum adsorption percentage of Rh-B by AHANC was

found as 83.20% at 0.025 g of AHANC stirred with 50 mL/25 ppm solution Rh-B dye solution about 60 min on pH 6. The adsorbent is investigated through particle analyzer, Brunauer-Emmett-Teller (BET), X-ray diffraction (XRD), Spectroscopy of Fourier Transform Infrared (FTIR), and Scanning electron microscope (SEM) with Energy dispersive X-ray (EDX) revealed important adsorption characteristics present in this low cost adsorbent. The isotherms of Freundlich, Langmuir, Temkin, Hurkins-Jura, Halsay, Radlich-Peterson, Dubinin-Radushkevich, Jovanovic, and Brunauer-Emmett-Teller were used in fitting equilibrium data. The isothermal data's were fine fitted with the Langmuir isothermal with the maximum capacity of adsorption for the monolayer was originate as 204.11 mg/g, at 40°C. The pseudo-second order kinetics, Elovich equation and also intra-particle diffusion methods through kinetic studies displayed the datas are well

explained by pseudo second order kinetics with a very good regression-coefficient close to 1 and mechanism of intra-particle diffusion involved rate controlling step of adsorption. The thermodynamic parameters are the negative value of $\Delta G°$ denotes the spontaneity of adsorption mechanism of Rh-B and $\Delta H°$ & $\Delta S°$ positive value displays endothermic character.

ACKNOWLEDGEMENT

Conflict interest
The author declares that we have no conflict of interest.

REFERENCES

1. Singh S.; Kumar A.; Gupta H.; *Applied Water Science.*, **2020**, *10*(8), 185, 1-8.

2. Wong S.; Ghafar N.A.; Ngadi N.; Razmi F.A.; Inuwa I.M.; Mat R.; Amin N.A.S.; *Scientific Reports.*, **2020**, *10*(1), 2928, 1-13.

3. Abdolrahimi N.; Tadjarodi A.; *Proceedings.*, **2019**, *41*(1), 51, 1-4.

4. Jinendra U.; Bilehal D.; Nagabhushana B.M.; Kumar A.P.; *Heliyon.*, **2021**, *7*(4), e06851, 1-9.

5. Bello O.S.; Alabi E.O.; Adegoke K.A.; Adegboyega S.A.; Inyinbor A.A.; Dada A.O.; *Heliyon.*, **2020**, *6*(1), e02872, 1-13.

6. Li A.; Huang W.; Qiu N.; Mou F.; Wang F.; *Materials Research Express.*, **2020**, *7*(5), 055505, 1-13.

7. Oyekanmi A.A.; Ahmad A.; Hossain K.; Rafatullah M.; *PLoS ONE.*, **2019**, *14*(5), e0216878, 1-20.

8. Bello O.S.; Adegoke K.A.; Inyinbor A.A.; Dada A.O.; *Water Environment Research.*, **2021**, *93*(10), 2308-2328.

9. Zhao Y.; Yang H.; Sun J.; Zhang Y.; Xia S.; *ACS Omega.*, **2021**, *6*(26), 17086–17094.

10. Aslam Z.; Yousaf I.; Zahir A.; Akhtar A.; *Turkish Journal of Chemistry.*, **2021**, *45*(4), 1189-1200.

11. Baddouh A.; Brahim E.I.; Elhassan A.; Mohamed M.R.; Lahcen B.; Hilali M.; *Journal of Chemistry.*, **2019**, Article ID: 1424797, 1-10.

12. Alakhras F.; Ouachtak H.; Alhajri E.; Rehman R.; Al-Mazaideh G.; Anastopoulos I.; Lima E.C.; *Separation Science and Technology.*, **2021**, *57*(4), 542-554.

13. Du J.; Yang X.; Xiong H.; Dong Z.; Wang Z.; Chen Z.; Zhao L.; *Journal of Chemical & Engineering Data.*, **2021**, *66*(3), 1264–1272.

14. Al-Gheethi A.A.; Azhar Q.M.; Senthil Kumar P.; Yusuf A.A.; Al-Buriahi A.K.; Radin Mohamed R.M.S.; Al-shaibani M.M.; *Chemosphere.*, **2022**, *287*, 132080, 1-11.

15. Alhogbi B.G.; Altayeb S.; Bahaidarah E.A.; Zawrah M.F.; *Processes.*, **2021**, *9*(3) 416, 1-20.

16. Geng J.; Gu F.; Chang J.M.; *Journal of Hazardous Materials.*, **2019**, *375*, 174–181.

17. Chen X.; Li H.; Liu W.; Zhang X.; Wu Z.; Bi S.; Zhang W.; Zhan H.; Colloids and Surfaces A: *Physicochemical and Engineering Aspects.*, **2019**, *583*, 123976, 1-9.

18. Li Y.; Yan X.; Hu X.; Feng R.; Zhou M.; *Chemical Engineering Journal.*, **2019**, *375*, 122003, 1-7.

19. Saleh T.A.; Ali I.; *Journal of Environmental Chemical Engineering.*, **2018**, *6*(4), 5361–5368.

20. Rubab R.; Ali S.; Rehman A.U.; Khan S.A.; Khan A.M.; *Colloids and Surfaces A: Physicochemical and Engineering Aspects.*, **2021**, *615*, 126253, 1-10.